Directional Modulation Design Under Maximum and Minimum Magnitude Constraints for Weight Coefficients[☆]

Bo Zhang[a,*], Wei Liu[b], Yang Li[a], Xiaonan Zhao[a], Cheng Wang[a]

[a] *Tianjin Key Laboratory of Wireless Mobile Communications and Power Transmission, College of Electronic and Communication Engineering, Tianjin Normal University, Tianjin, 300387, China*

[b] *Communications Research Group, Department of Electronic and Electrical Engineering, University of Sheffield, Sheffield, S1 4ET, United Kingdom*

Abstract

Directional modulation (DM) as a physical layer security technique has been studied widely to meet different design requirements, such as minimum spacing between adjacent antennas, and robust against steering vector errors. However, weight magnitude constraints in DM area have not been studied thoroughly. In this paper, the possibility of imposing various weight magnitude constraints is explored and simultaneous maximum and minimum magnitude constraints for weight coefficients are proposed in DM design for the first time. The proposed maximum magnitude constraint can avoid the use of multiple-stage power amplifiers, and the minimum magnitude constraint can make sure a minimum power requirement for each antenna is achieved so that a reasonable minimum transmission range of the system can be maintained by effectively using all employed antennas. Since the resultant problem is non-convex, a solution to transform it into a convex form is described, allowing the problem to be solved conveniently using existing convex optimisation toolboxes. Design examples are provided to show the effectiveness of the proposed design.

Keywords: Directional modulation, linear antenna array, maximum magnitude constraint, minimum magnitude constraint.

[☆]The work was partially supported by Natural Science Foundation of Tianjin (18JCYBJC86000, 18JCYBJC86400), Science & Technology Development Fund of Tianjin Education Commission for Higher Education (2018KJ153).

[*]Corresponding author

Email addresses: b.zhangintj@tjnu.edu.cn (Bo Zhang), w.liu@sheffield.ac.uk (Wei Liu), liyang_tongxin@163.com (Yang Li), xiaonan5875@163.com (Xiaonan Zhao), cwang@tjnu.edu.cn (Cheng Wang)

1. Introduction

The Fifth Generation (5G) network has been studied widely [1, 2]. As a critical technique in 5G, beamforming can be used to protect data by keeping maximum power to desired direction or directions, while reducing power as low as possible for the rest of directions. However, it is possible for eavesdroppers in undesired directions to decode the transmitted signal, since the same constellation mappings are transmitted in all spatial angles. To solve the problem, directional modulation (DM) technique has been introduced, which keeps the main beam pointing to the desired direction or directions with known constellation mappings, while lowering the power and scrambling constellation points for the remaining directions simultaneously [3].

In [3], a parasitic array was applied to achieve DM in the near-field by changing the effective length of reflectors, while in the far-field, both reconfigurable antenna array [4] and phased antenna array [5, 6] were employed. For the reconfigurable antenna array design, DM was achieved by switching elements for each symbol, while for the phased antenna array design, DM was implemented by setting the phases and magnitudes of weight coefficients properly. To reduce the number of antennas of an antenna array, l_1 norm minimisation and reweighted l_1 norm minimisation methods were proposed for sparse antenna array designs [7]. An inherent limitation of DM is that eavesdroppers and the desired users can receive the same signal when they are in the same spatial direction of the antenna array; to overcome this limit, reflecting surfaces [8] and multiple antenna arrays [9] were introduced. Crossed-dipole antenna array for orthogonal polarisations [10] and inverse Discrete Fourier Transform (IDFT) for multiple signals transmission [11, 12] were presented for increasing channel capacity. In [13], directional antennas were used in the design instead of isotropic antennas, and a narrower low bit error rate (BER) range was achieved. In [14], dual beam DM method was introduced, followed by the BER DM synthesis method [15], pattern synthesis approach [16, 17] and time-modulated antenna array method [18]. Recently, artificial noise (AN) for DM was proposed to further advanced the directional modulation technology. Two methods to generate AN were introduced. One is the orthogonal vector method [19, 20], and the other is the AN projection matrix method [21, 22].

However, to our best knowledge, magnitude constraints have not been considered in this context. In the DM design, without maximum magnitude constraint, the magnitudes of coefficients could be very high on some antennas; this could cause serious problems in practice as high magnitude of signal needs multiple-stage power amplifiers. On the other hand, sometimes a minimum magnitude constraint is also necessary. For example, we want to make sure the transmission power of the whole antenna array meets a minimum threshold, ensuring its signal can travel over a required distance; since the maximum possible transmission power of the whole array is the squared sum of the magnitudes of all transmitted antenna signals, we may have to set a minimum transmission power for each employed antenna to reach this threshold. Therefore, in the paper, we consider the following two constraints simultaneously, i.e., maximum magnitude constraint and minimum magnitude constraint for weight coefficients.

The remaining part of this paper is structured as follows. A review of DM design based on a narrowband linear antenna array is given in Sec. 2. The proposed simultaneous maximum and minimum magnitude constraints for weight coefficients are introduced in Sec. 3, with a solution transforming the resultant non-convex problem into a convex form provided. In Sec. 4, design examples are provided, with conclusions drawn in Sec. 5.

2. Review of DM design based on narrowband linear antenna arrays

2.1. Narrowband beamforming

A narrowband linear antenna array with N omni-directional antennas for transmit beamforming is shown in Fig. 1. The weight coefficients and the spacing between the first antenna to its subsequent antennas are represented by w_n ($n = 0, 1, \ldots, N-1$) and d_n for $n = 1, \ldots, N-1$, respectively. The spatial angle $\theta \in [0^\circ, 180^\circ]$. The steering vector of the array is given by

$$\mathbf{s}(\omega, \theta) = [1, e^{j\omega d_1 \cos\theta/c}, \ldots, e^{j\omega d_{N-1} \cos\theta/c}]^T, \tag{1}$$

where $\{\cdot\}^T$ is the transpose operation, and c is the speed of propagation. For a uniform linear antenna array (ULA) with a half-wavelength spacing between adjacent antennas, where $d_n - d_{n-1} = \lambda/2$, the steering vector can be represented by

$$\mathbf{s}(\omega, \theta) = [1, e^{j\pi\cos\theta}, \ldots, e^{j\pi(N-1)\cos\theta}]^T. \tag{2}$$

$\mathbf{w}$ can be used as a weight vector including all weight coefficients

$$\mathbf{w} = [w_0, w_1, \ldots, w_{N-1}]^T. \tag{3}$$

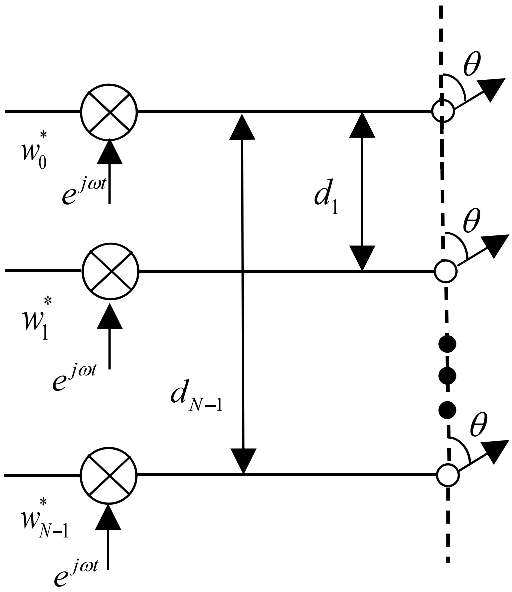

Figure 1: A narrowband transmit beamforming structure.

Then, the beam response of the array is given by

$$p(\omega,\theta) = \mathbf{w}^H \mathbf{s}(\omega,\theta), \tag{4}$$

where $\{\cdot\}^H$ represents the Hermitian transpose.

2.2. Directional modulation design

The way to achieve DM is to find the corresponding sets of weight coefficients for all symbols. For M-ary signaling, such as multiple phase shift keying (MPSK), there are M sets of desired array responses. Without loss of generality, we assume each desired responses include r mainlobe responses and $R-r$ sidelobe responses. Then for the m-th symbol ($m = 0, 1, \ldots, M-1$), we have

$$\begin{aligned} \mathbf{p}_{m,ML} &= [p_m(\omega,\theta_0), p_m(\omega,\theta_1), \ldots, p_m(\omega,\theta_{r-1})], \\ \mathbf{p}_{m,SL} &= [p_m(\omega,\theta_r), p_m(\omega,\theta_{r+1}), \ldots, p_m(\omega,\theta_{R-1})]. \end{aligned} \tag{5}$$

Similarly, the steering vector for mainlobe and sidelobe ranges can be given by

$$\begin{aligned} \mathbf{S}_{ML} &= [\mathbf{s}(\omega,\theta_0), \mathbf{s}(\omega,\theta_1), \ldots, \mathbf{s}(\omega,\theta_{r-1})], \\ \mathbf{S}_{SL} &= [\mathbf{s}(\omega,\theta_r), \mathbf{s}(\omega,\theta_{r+1}), \ldots, \mathbf{s}(\omega,\theta_{R-1})]. \end{aligned} \tag{6}$$

Note that all symbols for a fixed θ share the same steering vector. The corresponding weight vector can be represented by

$$\mathbf{w}_m = [w_{m,0}, w_{m,1}, \ldots, w_{m,N-1}]^T, \quad m = 0, 1, \ldots, M-1. \tag{7}$$

Based on the above parameters, for the m-th symbol, the corresponding weight coefficients for DM design can be obtained by solving the following problem

$$\begin{aligned} \min \quad & ||\mathbf{p}_{m,SL} - \mathbf{w}_m^H \mathbf{S}_{SL}||_2 \\ \text{subject to} \quad & \mathbf{w}_m^H \mathbf{S}_{ML} = \mathbf{p}_{m,ML}, \end{aligned} \tag{8}$$

where $||\cdot||_2$ denotes the l_2 norm. The cost function is to minimise the difference between desired and designed sidelobe responses, and the equality constraint is to make sure that the designed mainlobe responses are the same as desired ones.

3. The proposed maximum and minimum magnitude constraints for weight coefficients

One potential issue with the design in (8) is that the magnitudes of weight coefficients are not constrained. As mentioned earlier, in some applications, simultaneous maximum magnitude and minimum magnitude constraints for the DM design are needed, which will be discussed in the following.

For constraining the maximum magnitude of weight coefficient, we can use the following constraint

$$|w_{m,n}| \leq \delta_m, \tag{9}$$

for all n, where $|\cdot|$ represents the absolute value, and δ_m is the maximum magnitude threshold for the m-th set of weight coefficients. Similarly, the minimum magnitude constraint for weight coefficient is given by

$$|w_{m,n}| \geq \gamma_m, \tag{10}$$

where γ_m represents the minimum magnitude threshold. Then, the DM design under simultaneous maximum and minimum magnitude constraints for weight coefficient is given by

$$\begin{aligned} \min \quad & ||\mathbf{p}_{m,SL} - \mathbf{w}_m^H \mathbf{S}_{SL}||_2 \\ \text{subject to} \quad & \mathbf{w}_m^H \mathbf{S}_{ML} = \mathbf{p}_{m,ML} \\ & |w_{m,n}| \leq \delta_m \\ & |w_{m,n}| \geq \gamma_m. \end{aligned} \tag{11}$$

However, the second inequality constraints $|w_{m,n}| \geq \gamma_m$ is non-convex. To transform the non-convex problem into a convex one, the idea is that we set an equality constraint for the sum of all magnitudes of coefficients, and by keeping all magnitudes no greater than a given threshold, no magnitudes will be smaller than the minimum value; otherwise, the equality constraint will not be achieved.

First we assume that the magnitudes of all desired responses in the mainlobe directions are the same, i.e.,

$$|p_m(\omega, \theta_0)| = |p_m(\omega, \theta_1)| = \ldots = |p_m(\omega, \theta_{r-1})|. \tag{12}$$

We then use the following constraints

$$||\mathbf{w}_m||_1 \leq |p_m(\omega, \theta_0)|, \tag{13}$$

$$||\mathbf{w}_m||_\infty \leq \frac{|p_m(\omega, \theta_0)| - \gamma_m}{N-1}, \tag{14}$$

to replace the inequality constraint $|w_{m,n}| \geq \gamma_m$ in (11), where $||\cdot||_1$ represents the l_1 norm, and $||\cdot||_\infty$ represents the l_∞ norm.

The constraint (13) sets the sum of all magnitudes no greater than $|p_m(\omega, \theta_0)|$. With the following equality constraint

$$\mathbf{w}_m^H \mathbf{S}_{ML} = \mathbf{p}_{m,ML}, \tag{15}$$

(13) and (15) together set the sum of all magnitudes equal to $|p_m(\omega, \theta_0)|$, i.e.,

$$||\mathbf{w}_m||_1 = |p_m(\omega, \theta_0)|. \tag{16}$$

To prove it, we first analyse (15) based on (12),

$$\begin{aligned}
&\mathbf{w}_m^H \mathbf{S}_{ML} = \mathbf{p}_{m,ML} \\
\Rightarrow &\mathbf{w}_m^H \mathbf{s}(\omega, \theta_0) = p_m(\omega, \theta_0) \\
\Rightarrow &|\mathbf{w}_m^H \mathbf{s}(\omega, \theta_0)| = |p_m(\omega, \theta_0)| \\
= &|w_{m,0}^* + w_{m,1}^* e^{j\omega d_1 \cos\theta_0/c} + \ldots + w_{m,N-1}^* e^{j\omega d_{N-1} \cos\theta_0/c}| \\
\leq &|w_{m,0}^*| + |w_{m,1}^* e^{j\omega d_1 \cos\theta_0/c}| + \ldots + |w_{m,N-1}^* e^{j\omega d_{N-1} \cos\theta_0/c}| \\
\leq &|w_{m,0}^*| + |w_{m,1}^*| \cdot |e^{j\omega d_1 \cos\theta_0/c}| + \ldots + |w_{m,N-1}^*| \cdot |e^{j\omega d_{N-1} \cos\theta_0/c}| \\
\leq &|w_{m,0}^*| + |w_{m,1}^*| + \ldots + |w_{m,N-1}^*| \\
\leq &||\mathbf{w}_m||_1 \\
\Rightarrow &|p_m(\omega, \theta_0)| \leq ||\mathbf{w}_m||_1.
\end{aligned} \tag{17}$$

Then, based on (13) and (17), we can deduce (16).

The inequality constraint (14) makes sure that the entry of the vector $\mathbf{w}_m$ with the maximum magnitude is no greater than $\frac{|p_m(\omega,\theta_0)|-\gamma_m}{N-1}$. To derive it, we first assume the minimum magnitude of one entry is γ_m, and then the maximum sum of the remaining $(N-1)$ coefficients is $|p_m(\omega,\theta_0)|-\gamma_m$. To keep no entries from the $N-1$ coefficients smaller than γ_m, the maximum value is set to $\frac{|p_m(\omega,\theta_0)|-\gamma_m}{N-1}$.

Moreover, γ_m is not a random value, and there is a range for it,

$$\gamma_m \le \frac{|p_m(\omega,\theta_0)|}{N}. \tag{18}$$

If γ_m is greater than $\frac{|p_m(\omega,\theta_0)|}{N}$, e.g.,

$$\gamma_m = \frac{|p_m(\omega,\theta_0)|}{N} + \beta_m, \tag{19}$$

where β_m is a positive value, then by replacing γ_m in (14) by (19), we have

$$\begin{aligned} ||\mathbf{w}_m||_\infty &\le \frac{|p_m(\omega,\theta_0)| - (\frac{|p_m(\omega,\theta_0)|}{N} + \beta_m)}{N-1} \\ &\le \frac{|p_m(\omega,\theta_0)| - (\frac{|p_m(\omega,\theta_0)|+N\beta_m}{N})}{N-1} \\ &\le \frac{N|p_m(\omega,\theta_0)| - |p_m(\omega,\theta_0)| - N\beta_m}{N(N-1)} \\ &\le \frac{(N-1)|p_m(\omega,\theta_0)| - N\beta_m}{N(N-1)} \\ &\le \frac{|p_m(\omega,\theta_0)|}{N} - \frac{\beta_m}{N-1}. \end{aligned} \tag{20}$$

Then, even if the magnitudes of all coefficients take the maximum value, we have

$$\begin{aligned} ||\mathbf{w}_m||_1 &= (\frac{|p_m(\omega,\theta_0)|}{N} - \frac{\beta_m}{N-1})N \\ &= |p_m(\omega,\theta_0)| - \frac{N\beta_m}{N-1} \\ &< |p_m(\omega,\theta_0)| \end{aligned} \tag{21}$$

which does not satisfy (16).

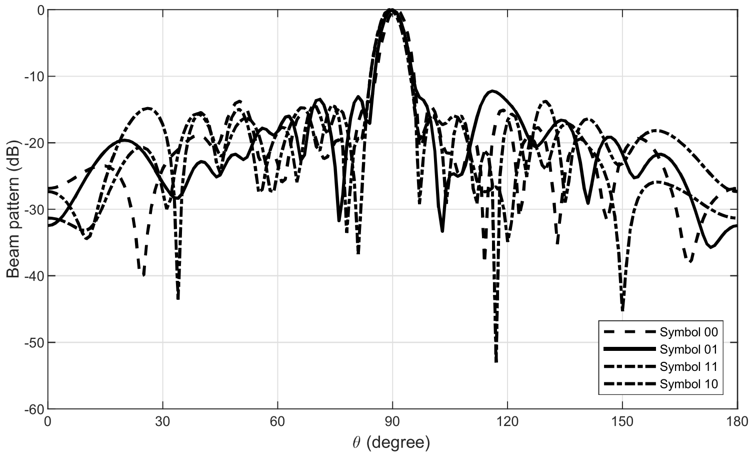

Figure 2: Resultant beam responses for the broadside design without magnitude constraints in (8).

As a result, the DM design under the maximum and minimum magnitude constraints for weight coefficients can be modified into

$$\begin{aligned} \min \quad & ||\mathbf{p}_{m,SL} - \mathbf{w}_m^H \mathbf{S}_{SL}||_2 \\ \text{subject to} \quad & \mathbf{w}_m^H \mathbf{S}_{ML} = \mathbf{p}_{m,ML} \\ & |w_{m,n}| \leq \delta_m \\ & ||\mathbf{w}_m||_1 \leq |p_m(\omega, \theta_0)| \\ & ||\mathbf{w}_m||_\infty \leq \frac{|p_m(\omega, \theta_0)| - \gamma_m}{N-1}. \end{aligned} \tag{22}$$

The above problem (22) can be solved by the CVX toolbox in MATLAB [23, 24].

Note that the proposed maximum and minimum magnitude constraints are set and calculated for each symbol. If the magnitudes of symbols are not the same, such as 16QAM, according to equation (22), $|p_m(\omega, \theta_0)|$ has to be changed, while the other two variables γ_m and N stay the same.

4. Design examples

In this section, both broadside and off-broadside designs are considered. For the broadside design, without loss of generality, we assume one mainlobe direction $\theta_{ML} = 90°$, and $\theta_{SL} \in [0°, 85°] \cup [95°, 180°]$. Similarly, for the off-broadside design, $\theta_{ML} = 60°$, and $\theta_{SL} \in [0°, 55°] \cup [65°, 180°]$. All design

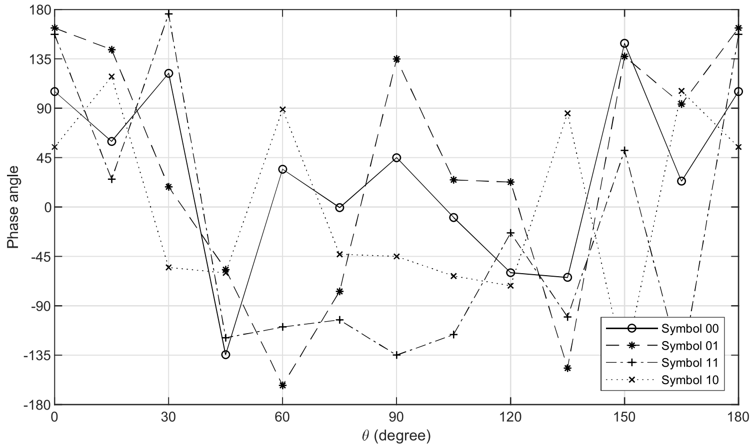

Figure 3: Resultant phase responses for the broadside design without magnitude constraints in (8).

Table 1: Magnitude of weight coefficients for the broadside design without magnitude constraints in (8) for symbol '00' ($m = 0$).

Weight	Magnitude	Weight	Magnitude	Weight	Magnitude
$w_{m,0}$	0.0412	$w_{m,7}$	0.0647	$w_{m,14}$	0.0573
$w_{m,1}$	0.0568	$w_{m,8}$	0.0532	$w_{m,15}$	0.0725
$w_{m,2}$	0.0128	$w_{m,9}$	0.0666	$w_{m,16}$	0.0549
$w_{m,3}$	0.0130	$w_{m,10}$	0.0817	$w_{m,17}$	0.0592
$w_{m,4}$	0.0674	$w_{m,11}$	0.0506	$w_{m,18}$	0.0519
$w_{m,5}$	0.0649	$w_{m,12}$	0.0635	$w_{m,19}$	0.0178
$w_{m,6}$	0.0592	$w_{m,13}$	0.0751		

Table 2: Magnitude of weight coefficients for the broadside design without magnitude constraints in (8) for symbol '01' ($m = 1$).

Weight	Magnitude	Weight	Magnitude	Weight	Magnitude
$w_{m,0}$	0.0406	$w_{m,7}$	0.0395	$w_{m,14}$	0.0360
$w_{m,1}$	0.0359	$w_{m,8}$	0.0547	$w_{m,15}$	0.0323
$w_{m,2}$	0.0474	$w_{m,9}$	0.0793	$w_{m,16}$	0.0434
$w_{m,3}$	0.0326	$w_{m,10}$	0.0728	$w_{m,17}$	0.0434
$w_{m,4}$	0.0890	$w_{m,11}$	0.0493	$w_{m,18}$	0.0284
$w_{m,5}$	0.1126	$w_{m,12}$	0.0250	$w_{m,19}$	0.0450
$w_{m,6}$	0.0832	$w_{m,13}$	0.0635		

Table 3: Magnitude of weight coefficients for the broadside design without magnitude constraints in (8) for symbol '11' ($m = 2$).

Weight	Magnitude	Weight	Magnitude	Weight	Magnitude
$w_{m,0}$	0.0442	$w_{m,7}$	0.0713	$w_{m,14}$	0.0603
$w_{m,1}$	0.0206	$w_{m,8}$	0.0881	$w_{m,15}$	0.0539
$w_{m,2}$	0.0471	$w_{m,9}$	0.0785	$w_{m,16}$	0.0687
$w_{m,3}$	0.0725	$w_{m,10}$	0.0558	$w_{m,17}$	0.0316
$w_{m,4}$	0.0215	$w_{m,11}$	0.0623	$w_{m,18}$	0.0097
$w_{m,5}$	0.0440	$w_{m,12}$	0.0528	$w_{m,19}$	0.0196
$w_{m,6}$	0.0850	$w_{m,13}$	0.0806		

Table 4: Magnitude of weight coefficients for the broadside design without magnitude constraints in (8) for symbol '10' ($m = 3$).

Weight	Magnitude	Weight	Magnitude	Weight	Magnitude
$w_{m,0}$	0.0570	$w_{m,7}$	0.0777	$w_{m,14}$	0.0468
$w_{m,1}$	0.0583	$w_{m,8}$	0.0804	$w_{m,15}$	0.0296
$w_{m,2}$	0.0414	$w_{m,9}$	0.0777	$w_{m,16}$	0.0582
$w_{m,3}$	0.0637	$w_{m,10}$	0.0551	$w_{m,17}$	0.0204
$w_{m,4}$	0.0429	$w_{m,11}$	0.0462	$w_{m,18}$	0.0349
$w_{m,5}$	0.0821	$w_{m,12}$	0.0574	$w_{m,19}$	0.0437
$w_{m,6}$	0.0754	$w_{m,13}$	0.0766		

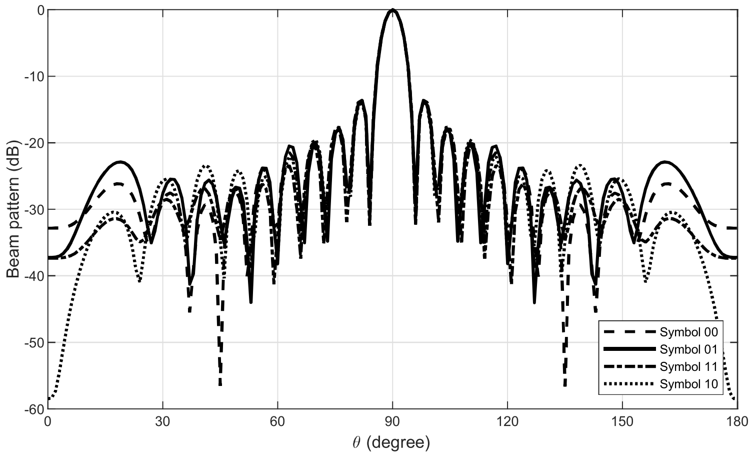

Figure 4: Resultant beam responses for the broadside design with magnitude constraints in (22).

examples are based on an $N = 20$ ULA. The desired response in the desired direction is a value of one (magnitude) with 90° phase shift (QPSK), i.e.,

$$\frac{\sqrt{2}}{2} + i\frac{\sqrt{2}}{2}, -\frac{\sqrt{2}}{2} + i\frac{\sqrt{2}}{2}, -\frac{\sqrt{2}}{2} - i\frac{\sqrt{2}}{2}, \frac{\sqrt{2}}{2} - i\frac{\sqrt{2}}{2} \tag{23}$$

for symbols '00', '01', '11', '10', and a value of 0.3 (magnitude) with random phase shifts over the sidelobe regions. The maximum magnitude threshold $\delta_m = 0.07$, and the minimum magnitude threshold $\gamma_m = 0.025$ for all $m = 0, 1, 2, 3$.

To verify the performance of the proposed design, the beam and phase patterns for the designs with and without magnitude constraints for weight coefficients are provided. BER is also calculated based on which quadrant the received complex-valued signal falls in. In this example, 10^6 bits are transmitted, with 12 dB signal to noise ratio (SNR) in the mainlobe direction, and the same additive white Gaussian noise (AWGN) power levels in all directions.

For the broadside design without magnitude constraints in (8), Figs. 2 and 3 show the beam and phase patterns for symbols '00, 01, 11, 10', where all main beams are exactly pointed to 90° (the desired direction) with a low sidelobe level, and the phases in the desired direction follow the standard QPSK constellation mappings, but random for the rest of the angles. However, as shown in Tables 1, 2, 3 and 4, magnitudes of eight weight coefficients are lower than the minimum magnitude threshold 0.025, e.g.,

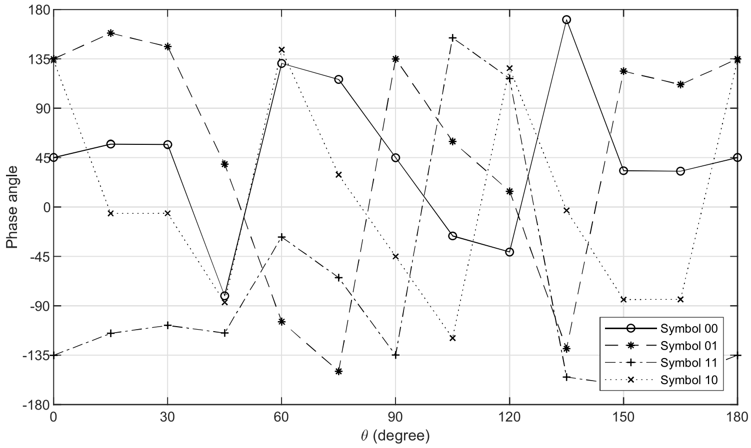

Figure 5: Resultant phase responses for the broadside design with magnitude constraints in (22).

Table 5: Magnitude of weight coefficients for the broadside design with magnitude constraints in (22) for symbol '00' ($m = 0$).

Weight	Magnitude	Weight	Magnitude	Weight	Magnitude
$w_{m,0}$	0.0513	$w_{m,7}$	0.0513	$w_{m,14}$	0.0513
$w_{m,1}$	0.0513	$w_{m,8}$	0.0513	$w_{m,15}$	0.0513
$w_{m,2}$	0.0496	$w_{m,9}$	0.0513	$w_{m,16}$	0.0513
$w_{m,3}$	0.0387	$w_{m,10}$	0.0513	$w_{m,17}$	0.0513
$w_{m,4}$	0.0513	$w_{m,11}$	0.0513	$w_{m,18}$	0.0513
$w_{m,5}$	0.0513	$w_{m,12}$	0.0513	$w_{m,19}$	0.0394
$w_{m,6}$	0.0513	$w_{m,13}$	0.0513		

Table 6: Magnitude of weight coefficients for the broadside design with magnitude constraints in (22) for symbol '01' ($m = 1$).

Weight	Magnitude	Weight	Magnitude	Weight	Magnitude
$w_{m,0}$	0.0513	$w_{m,7}$	0.0508	$w_{m,14}$	0.0513
$w_{m,1}$	0.0466	$w_{m,8}$	0.0513	$w_{m,15}$	0.0513
$w_{m,2}$	0.0513	$w_{m,9}$	0.0513	$w_{m,16}$	0.0513
$w_{m,3}$	0.0365	$w_{m,10}$	0.0513	$w_{m,17}$	0.0513
$w_{m,4}$	0.0513	$w_{m,11}$	0.0513	$w_{m,18}$	0.0513
$w_{m,5}$	0.0513	$w_{m,12}$	0.0450	$w_{m,19}$	0.0513
$w_{m,6}$	0.0513	$w_{m,13}$	0.0513		

Table 7: Magnitude of weight coefficients for the broadside design with magnitude constraints in (22) for symbol '11' ($m = 2$).

Weight	Magnitude	Weight	Magnitude	Weight	Magnitude
$w_{m,0}$	0.0513	$w_{m,7}$	0.0513	$w_{m,14}$	0.0513
$w_{m,1}$	0.0513	$w_{m,8}$	0.0513	$w_{m,15}$	0.0513
$w_{m,2}$	0.0513	$w_{m,9}$	0.0513	$w_{m,16}$	0.0513
$w_{m,3}$	0.0513	$w_{m,10}$	0.0513	$w_{m,17}$	0.0513
$w_{m,4}$	0.0449	$w_{m,11}$	0.0513	$w_{m,18}$	0.0513
$w_{m,5}$	0.0513	$w_{m,12}$	0.0513	$w_{m,19}$	0.0514
$w_{m,6}$	0.0513	$w_{m,13}$	0.0513		

Table 8: Magnitude of weight coefficients for the broadside design with magnitude constraints in (22) for symbol '10' ($m = 3$).

Weight	Magnitude	Weight	Magnitude	Weight	Magnitude
$w_{m,0}$	0.0513	$w_{m,7}$	0.0513	$w_{m,14}$	0.0513
$w_{m,1}$	0.0513	$w_{m,8}$	0.0513	$w_{m,15}$	0.0513
$w_{m,2}$	0.0513	$w_{m,9}$	0.0513	$w_{m,16}$	0.0513
$w_{m,3}$	0.0513	$w_{m,10}$	0.0513	$w_{m,17}$	0.0440
$w_{m,4}$	0.0376	$w_{m,11}$	0.0513	$w_{m,18}$	0.0513
$w_{m,5}$	0.0513	$w_{m,12}$	0.0513	$w_{m,19}$	0.0461
$w_{m,6}$	0.0513	$w_{m,13}$	0.0513		

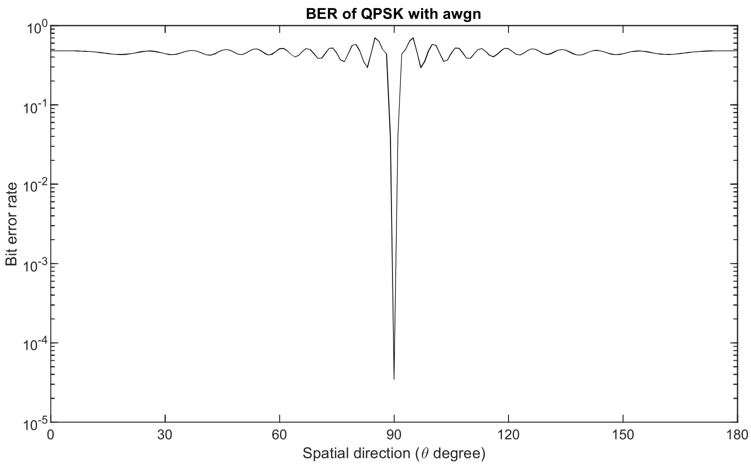

Figure 6: BER for the broadside design with magnitude constraints in (22).

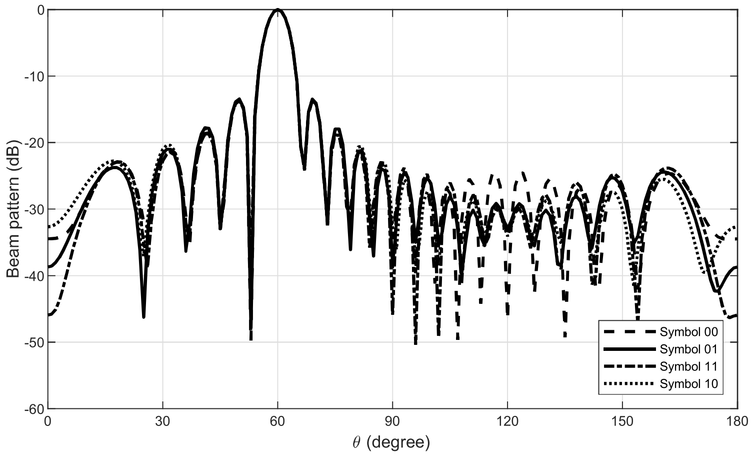

Figure 7: Resultant beam responses for the off-broadside design with magnitude constraints in (22).

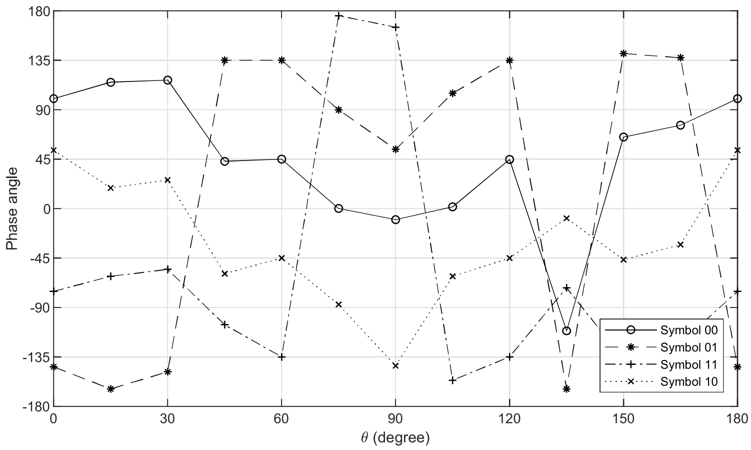

Figure 8: Resultant phase responses for the off-broadside design with magnitude constraints in (22).

Table 9: Magnitude of weight coefficients for the off-broadside design with magnitude constraints in (22) for symbol '00' ($m = 0$).

Weight	Magnitude	Weight	Magnitude	Weight	Magnitude
$w_{m,0}$	0.0513	$w_{m,7}$	0.0513	$w_{m,14}$	0.0513
$w_{m,1}$	0.0513	$w_{m,8}$	0.0513	$w_{m,15}$	0.0513
$w_{m,2}$	0.0513	$w_{m,9}$	0.0513	$w_{m,16}$	0.0513
$w_{m,3}$	0.0439	$w_{m,10}$	0.0512	$w_{m,17}$	0.0513
$w_{m,4}$	0.0513	$w_{m,11}$	0.0513	$w_{m,18}$	0.0406
$w_{m,5}$	0.0513	$w_{m,12}$	0.0513	$w_{m,19}$	0.0432
$w_{m,6}$	0.0513	$w_{m,13}$	0.0513		

Table 10: Magnitude of weight coefficients for the off-broadside design with magnitude constraints in (22) for symbol '01' ($m = 1$).

Weight	Magnitude	Weight	Magnitude	Weight	Magnitude
$w_{m,0}$	0.0513	$w_{m,7}$	0.0508	$w_{m,14}$	0.0513
$w_{m,1}$	0.0513	$w_{m,8}$	0.0513	$w_{m,15}$	0.0513
$w_{m,2}$	0.0495	$w_{m,9}$	0.0513	$w_{m,16}$	0.0513
$w_{m,3}$	0.0513	$w_{m,10}$	0.0513	$w_{m,17}$	0.0502
$w_{m,4}$	0.0513	$w_{m,11}$	0.0513	$w_{m,18}$	0.0513
$w_{m,5}$	0.0459	$w_{m,12}$	0.0450	$w_{m,19}$	0.0333
$w_{m,6}$	0.0513	$w_{m,13}$	0.0513		

Table 11: Magnitude of weight coefficients for the off-broadside design with magnitude constraints in (22) for symbol '11' ($m = 2$).

Weight	Magnitude	Weight	Magnitude	Weight	Magnitude
$w_{m,0}$	0.0513	$w_{m,7}$	0.0513	$w_{m,14}$	0.0513
$w_{m,1}$	0.0513	$w_{m,8}$	0.0513	$w_{m,15}$	0.0513
$w_{m,2}$	0.0513	$w_{m,9}$	0.0513	$w_{m,16}$	0.0513
$w_{m,3}$	0.0513	$w_{m,10}$	0.0513	$w_{m,17}$	0.0416
$w_{m,4}$	0.0513	$w_{m,11}$	0.0513	$w_{m,18}$	0.0488
$w_{m,5}$	0.0513	$w_{m,12}$	0.0513	$w_{m,19}$	0.0372
$w_{m,6}$	0.0513	$w_{m,13}$	0.0513		

Table 12: Magnitude of weight coefficients for the off-broadside design with magnitude constraints in (22) for symbol '10' ($m = 3$).

Weight	Magnitude	Weight	Magnitude	Weight	Magnitude
$w_{m,0}$	0.0513	$w_{m,7}$	0.0513	$w_{m,14}$	0.0513
$w_{m,1}$	0.0513	$w_{m,8}$	0.0513	$w_{m,15}$	0.0513
$w_{m,2}$	0.0513	$w_{m,9}$	0.0513	$w_{m,16}$	0.0513
$w_{m,3}$	0.0471	$w_{m,10}$	0.0513	$w_{m,17}$	0.0513
$w_{m,4}$	0.0480	$w_{m,11}$	0.0513	$w_{m,18}$	0.0513
$w_{m,5}$	0.0513	$w_{m,12}$	0.0513	$w_{m,19}$	0.0325
$w_{m,6}$	0.0513	$w_{m,13}$	0.0513		

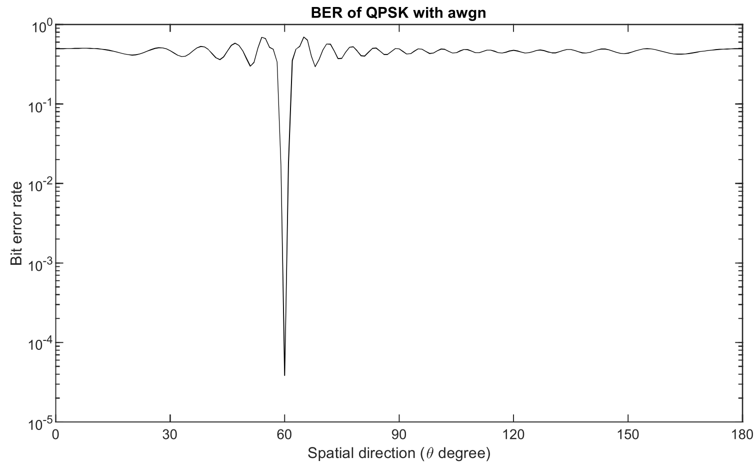

Figure 9: BER for the off-broadside design with magnitude constraints in (22).

$w_{0,2}$, $w_{0,3}$, $w_{0,19}$, and magnitudes of 20 weight coefficients are higher than the maximum magnitude threshold 0.07, e.g., $w_{0,10}$, $w_{0,13}$, $w_{0,15}$, representing unsatisfactory designs.

In contrast, for the broadside design with the maximum and minimum magnitude constraints in (22), Figs. 4 and 5 show the corresponding beam and phase patterns, meeting the needs of the DM design. The magnitudes of the m-th set of weight coefficients for $m = 0, 1, 2, 3$ are shown in Tables 5, 6, 7 and 8, respectively, where all magnitudes satisfy $0.025 \leq w_{m,n} \leq 0.07$. The BER performance of the proposed design is given in Fig. 6, with a very small value (10^{-5}) in the desired direction (90°), and a value of about 0.5 in other directions, demonstrating the effectiveness of the proposed design (22).

For the off-broadside design, with the proposed magnitude constraints in (22), the corresponding beam and phase patterns are shown in Figs. 7 and 8; the magnitudes of all weight coefficients $w_{m,n} \in [0.025, 0.07]$ for all $m = 0, 1, 2, 3$, and $n = 0, 1, \ldots, 19$, are displayed in Tables 9, 10, 11 and 12; the corresponding BER performance is given in Fig. 9, all demonstrating a satisfactory design.

5. Conclusions

Directional modulation design under simultaneous maximum and minimum magnitude constraints for weight coefficients has been studied for the first time, and a solution to transform the resultant non-convex constant magnitude constraint into a convex form was described, allowing the problem to be solved conveniently by existing toolboxes. The proposed maximum magnitude constraint can avoid the use of multiple-stage power amplifiers, and the minimum magnitude constraint can make sure a minimum power requirement for each antenna is achieved so that a reasonable minimum transmission range of the system can be maintained by effectively using all employed antennas. As shown in the provided design examples, based on the given beam pattern, phase pattern, BER and Tables for weight coefficients' magnitudes, the proposed design works well for both broadside and off-broadside DM scenarios.

Reference

[1] X. Liu, M. Jia, X. Zhang, and W. Lu, "A novel multichannel internet of things based on dynamic spectrum sharing in 5g communication,"

IEEE Internet of Things Journal, vol. 6, no. 4, pp. 5962–5970, Augu 2019.

[2] X. Liu and X. Zhang, "Rate and energy efficiency improvements for 5G-based IoT with simultaneous transfer," *IEEE Internet of Things Journal*, vol. 6, no. 4, pp. 5971–5980, August 2019.

[3] A. Babakhani, D. B. Rutledge, and A. Hajimiri, "Near-field direct antenna modulation," *IEEE Microwave Magazine*, vol. 10, no. 1, pp. 36–46, February 2009.

[4] M. P. Daly and J. T. Bernhard, "Beamsteering in pattern reconfigurable arrays using directional modulation," *IEEE Transactions on Antennas and Propagation*, vol. 58, no. 7, pp. 2259–2265, March 2010.

[5] ——, "Directional modulation technique for phased arrays," *IEEE Transactions on Antennas and Propagation*, vol. 57, no. 9, pp. 2633–2640, September 2009.

[6] T. Xie, J. Zhu, and Y. Li, "Artificial-noise-aided zero-forcing synthesis approach for secure multi-beam directional modulation," *IEEE Communications Letters*, vol. PP, no. 99, pp. 1–1, 2017.

[7] B. Zhang, W. Liu, and X. Gou, "Compressive sensing based sparse antenna array design for directional modulation," *IET Microwaves, Antennas Propagation*, vol. 11, no. 5, pp. 634–641, April 2017.

[8] B. Zhang and W. Liu, "Antenna array based positional modulation with a two-ray multi-path model," in *Proc. Sensor Array and Multichannel signal processing workshop 2018 (SAM2018)*, Sheffield, UK, July 2018, to appear.

[9] B. Zhang and W. Liu, "Positional modulation design based on multiple phased antenna arrays," *IEEE Access*, vol. 7, pp. 33 898–33 905, 2019.

[10] B. Zhang, W. Liu, and X. Lan, "Orthogonally polarized dual-channel directional modulation based on crossed-dipole arrays," *IEEE Access*, vol. 7, pp. 34 198–34 206, 2019.

[11] B. Zhang and W. Liu, "Multi-carrier based phased antenna array design for directional modulation," *IET Microwaves, Antennas Propagation*, vol. 12, no. 5, pp. 765–772, April 2018.

[12] B. Zhang, W. Liu, and Q. Li, "Multi-carrier waveform design for directional modulation under peak to average power ratio constraint," *IEEE Access*, pp. 1–1, 2019.

[13] H. Z. Shi and A. Tennant, "Enhancing the security of communication via directly modulated antenna arrays," *IET Microwaves, Antennas & Propagation*, vol. 7, no. 8, pp. 606–611, June 2013.

[14] T. Hong, M. Z. Song, and Y. Liu, "Dual-beam directional modulation technique for physical-layer secure communication," *IEEE Antennas and Wireless Propagation Letters*, vol. 10, pp. 1417–1420, December 2011.

[15] Y. Ding and V. Fusco, "Directional modulation transmitter synthesis using particle swarm optimization," in *Proc. Loughborough Antennas and Propagation Conference*, Loughborough, UK, November 2013, pp. 500–503.

[16] ——, "Directional modulation transmitter radiation pattern considerations," *IET Microwaves, Antennas & Propagation*, vol. 7, no. 15, pp. 1201–1206, December 2013.

[17] Y. Ding and V. F. Fusco, "Directional modulation far-field pattern separation synthesis approach," *IET Microwaves, Antennas Propagation*, vol. 9, no. 1, pp. 41–48, 2015.

[18] Q. J. Zhu, S. W. Yang, R. L. Yao, and Z. P. Nie, "Directional modulation based on 4-D antenna arrays," *IEEE Transactions on Antennas and Propagation*, vol. 62, no. 2, pp. 621–628, February 2014.

[19] Y. Ding and V. Fusco, "A vector approach for the analysis and synthesis of directional modulation transmitters," *IEEE Transactions on Antennas and Propagation*, vol. 62, no. 1, pp. 361–370, January 2014.

[20] Y. Ding and V. Fusco, "Vector representation of directional modulation transmitters," in *The 8th European Conference on Antennas and Propagation (EuCAP 2014)*, April 2014, pp. 367–371.

[21] J. Hu, F. Shu, and J. Li, "Robust synthesis method for secure directional modulation with imperfect direction angle," *IEEE Communications Letters*, vol. 20, no. 6, pp. 1084–1087, June 2016.

[22] J. Hu, S. Yan, F. Shu, J. Wang, J. Li, and Y. Zhang, "Artificial-noise-aided secure transmission with directional modulation based on random frequency diverse arrays," *IEEE Access*, vol. 5, pp. 1658–1667, 2017.

[23] M. Grant and S. Boyd, "Graph implementations for nonsmooth convex programs," in *Recent Advances in Learning and Control*, ser. Lecture Notes in Control and Information Sciences, V. Blondel, S. Boyd, and H. Kimura, Eds. Springer-Verlag Limited, 2008, pp. 95–110, http://stanford.edu/~boyd/graph$_$dcp.html.

[24] C. Research, "CVX: Matlab software for disciplined convex programming, version 2.0 beta," http://cvxr.com/cvx, September 2012.